CrossMark

ORIGINAL PAPER

Evaluation of relative tectonic activity of Buin Zahra-Avaj area, northern Iran

Masoome Alaei[1] · Maryam Dehbozorgi[1] · Mohammad R. Ghassemi[2] · Reza Nozaem[3]

Abstract Present active tectonics is affecting central Alborz and created various dynamic landforms in Buin Zahra-Avaj area, northern Iran. The area, located between the southern central Alborz and the edge of northwestern central Iran, is the result of both the Arabian–Eurasian convergence and clockwise rotation of the south Caspian Basin with respect to Eurasia in which most of the steep fault planes have a left lateral strike-slip component and most of the dip-slip faults are reverse, dipping SW. Since this region consists of several residential and industrial areas and includes several fault zones, the assessment of the structures of the present activity is vital. Six significant morphometric indices have been applied for this evaluation including stream length–gradient (SL), drainage basin asymmetry factor (Af), hypsometric integral (Hi), ratio of valley floor width to valley height (Vf), drainage basin shape (Bs), and mountain front sinuosity (Smf). The combined analyzed indices, represented through the relative tectonic activity (Iat), were used. The study area was divided into four regions according to the values of Iat. These classes include class 1 (very high activity, 18%), class 2 (high, 20%), class 3 (moderate, 44%), and class 4 (low, 18%). The results of these indices are consistent with field observations on landforms and the deformation of Quaternary deposits.

✉ Maryam Dehbozorgi
   M_Dehbozorgi@khu.ac.ir

[1] Department of Earth Science, Kharazmi University, Tehran, Iran

[2] Research Institute for Earth Sciences, Geological Survey of Iran, Tehran, Iran

[3] School of Geology, College of Science, University of Tehran, Tehran, Iran

Introduction

The Iranian Plateau is situated in the Alpine-Himalayan orogeny between the Eurasian plate in the north and the Arabian plate in the south. It is being shortened by the northward movement of the Arabian plate, which causes more parts of Iran to be active and dynamic in terms of tectonic movements (Berberian and King 1981; Allen et al. 2004, Allen and Armstrong 2008). The recent tectonic activity in the southern edge of central Alborz causes both the development and deformation of the landforms. Seismic records indicate a high frequency of earthquakes of relatively small magnitude (<4) and infrequent large earthquakes (>5.1) in the Alborz (Berberian and Yeats 2001). The south Qazvin plain has been the location of some of the great Iranian earthquakes. However, the lack of earthquake through some main fault segments restrains the possibility of seismic hazard evaluation. Researchers are of the opinion that the potential of generating an earthquake along different fault segments in large fault zones is not similar (Azor et al. 2002; Silva et al. 2003). Geomorphic indices, therefore, can be used to investigate active faults and seismic hazard although they should be coupled with field evidences. Considering the existence of residential and industrial regions and their development in the study area, the present state of knowledge does not appear sufficient, and morphotectonic studies seem to be really important. We used geomorphic indices of active tectonics that are known to be useful in active tectonic studies (Bull and McFadden 1977; Azor et al. 2002; Keller and Pinter 2002; Silva et al. 2003; Dehbozorgi et al. 2010, Troiani et al. 2014). In the recent studies related to morphotectonics, a

mixture of geomorphologic and morphometric analyses of landforms and topographic analyses is utilized to detect active tectonics (Della Seta et al. 2008). We analyzed six geomorphic indices: the stream length-gradient index (SL), drainage basin asymmetry factor (Af), hypsometric integral (Hi), valley floor width to valley height ratio (Vf), drainage basin shape (Bs), and mountain-front sinuosity (Smf). We then computed a single index (Iat) from the six indices to define a spatialized relative tectonic activity.

We tested the different classification methods in GIS and chose the best ones and the right number of classes based on data distribution for each index through the study area. We also examined the results of the morphometric analyses through field geomorphological observations.

Regional geology

The study basin is located at the southern central Alborz zone and northwestern central Iran zone, as some parts of the study area are located in Alborz and other parts are situated in the central Iran; its overall tectonics thoroughly follows both Alborz and central Iran tectonics. This region was affected by the northward convergence of central Iran toward Eurasia and to the northwestward motion of the South Caspian Basin with respect to Eurasia (Jackson et al. 2002; Ritz et al. 2006). With regard to the present-day deformation on the major active faults in the Iranian plateau, shortening has occurred since ~3–7 million years ago (Allen et al. 2004). Since that time, the continental collision has continued in the general NNE trending across the suture zone between the Arabian and Eurasian plates and at a rate of 22 mm/year based on GPS measurements (Vernant et al. 2004a). In central Iran, however, the shortening occurs in a N–S direction and with a rate of about 2 mm/year (Vernant et al. 2004a). The S–N contraction formed thrust faults prior to the Pliocene. After the Plio-Pleistocene sinistral strike-slip tectonics, the folding of the sedimentary covering and the development of thrust faults with a N–NE dip occurred by the diversion of convergence to the SW–NE direction in Phanerozoic sediments (Allen et al. 2003). Generally, the dominant tectonic features of the study area involve thrust faults. The Ipak fault is one of the major fault systems in the area (Berberian and King 1981), located about 120 km west of Tehran and responsible for the 1962 Buin Zahra earthquake of Ms 7.2 (Mw 7.0). The earthquake was associated with 95 km of surface rupture along the Ipak reverse fault with average throw of 140 cm and left-lateral displacement of 60 cm (Ambraseys 1963; Berberian 1983, Berberian et al. 1993). The other main faults of the basin are the Avaj and the Hasan Abad faults, in the west of the basin, and the Soltaniyeh fault in the northwest, which are shown in Fig. 1. The study area (11,673 km^2) is located in Shoor river basin which has divided in to 134 sub-basins, represented in

Fig. 2. The research aim is to analyze several different indices in sub-basins and classify them into tectonic classes based on the range of values of individual indices. The area shows the outcrop of a wide variety of sedimentary and metamorphic rock and unconsolidated sedimentary deposits, most of which range in age from Jurassic through Quaternary. The rocks vary greatly in composition, degree of consolidation, and depth of weathering. Marl, sandstone, and volcanic rocks predominate. We categorized the level of rock resistance based on rock types shown in Fig. 3 and field observations: low resistance (alluvial deposits, older alluvial fan deposit, Plio-Quaternary conglomerate, phyllite, schist, shale, marl, gypsum, and tuff) and high resistance (limestone, sandstone, dolomite, and hard conglomerate, and volcanic and plutonic rocks).

Morphometric analysis and geomorphic indices of tectonic activity

Some geomorphic indices have been developed to identify areas experiencing rapid tectonic deformation (Keller and Pinter 2002). Recently, in morphotectonic studies, traditional geomorphic analysis has been integrated with the morphometric analysis of landforms and with geostatistical topographic analysis (Cox 1994; Pike 2002; Della Seta 2004; Della Seta et al. 2004). Geomorphic indices useful for studying active tectonics include the stream length-gradient index (SL), drainage basin asymmetry (Af), hypsometric integral (Hi), valley floor width–valley height ratio (Vf), drainage basin shape (Bs), and mountain-front sinuosity (Smf) (Keller and Pinter 1996).

Stream length-gradient index

The development of topography results from an adjustment between uplift and the process of erosion as rivers flow over rocks and soils of variable strength (Hack 1973). The adjustment eventually reaches a dynamic equilibrium. This value is affected by the resistance of rocks, on the basis of field recognition and rock types shown in Fig. 3. The SL is defined by Eq. (1) (Hack 1973):

$$SL = \left(\Delta H \Big/ \Delta Lr \right) Lsc, \tag{1}$$

where ΔH is change in altitude, ΔLr is the length of a reach, and Lsc is the horizontal length from the watershed divide to midpoint of the reach. The SL index can be used to evaluate relative tectonic activity (Keller and Pinter 2002). Although an area on soft rocks with high SL values indicates recent tectonic activity, anomalously low values of SL may also represent such activity when rivers and streams flow through strike-slip faults. The quantities of the SL index were computed along the streams for all sub-basins. These values were calculated on
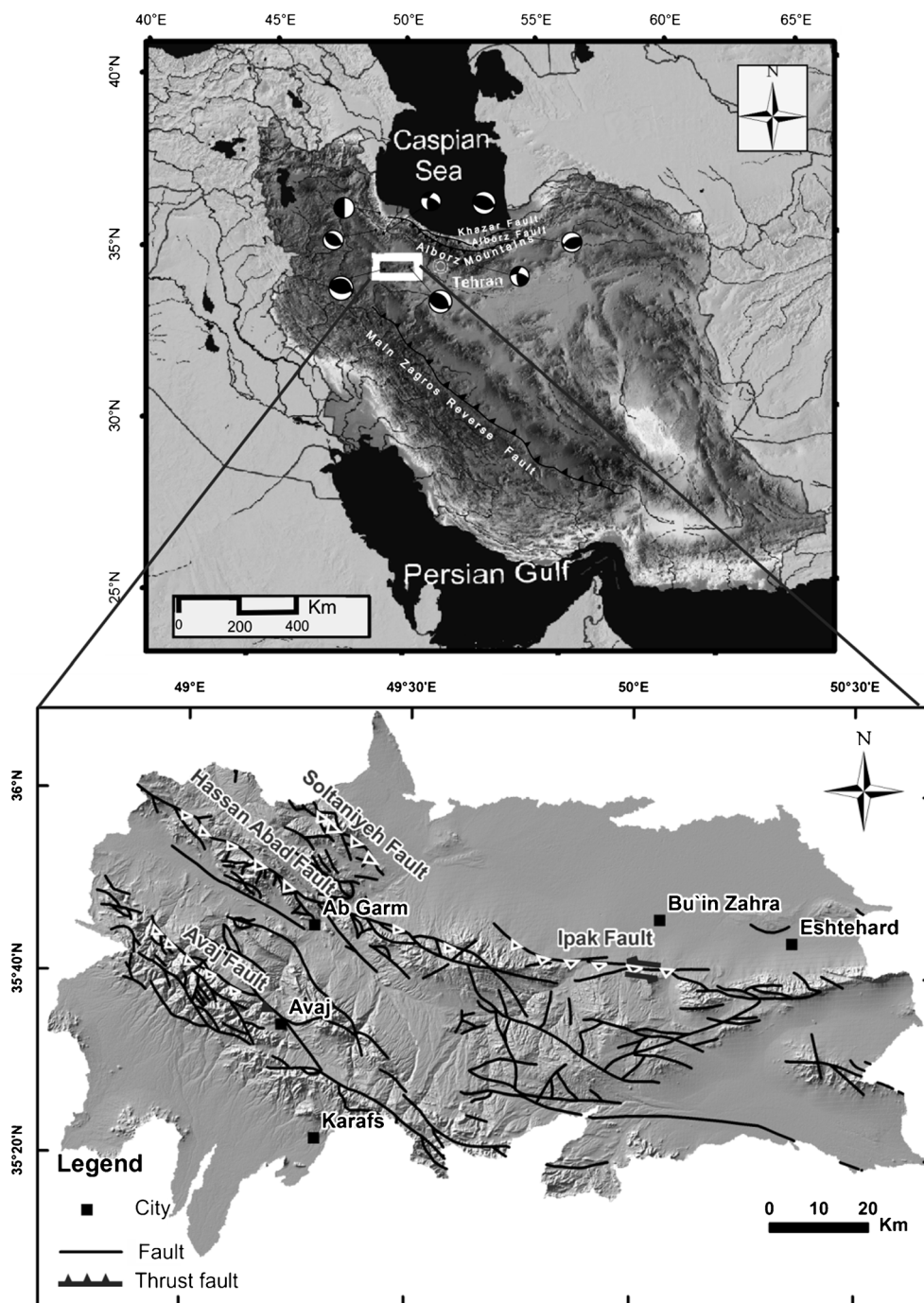
the DEM in GIS and the results are shown in Figs. 4, 5a, and 6. The high amount of this index along Hasan Abad, Avaj, and Ipak faults indicate high tectonic activity through the mentioned fault. The values were classified into three categories: 1 ($688 \leq SL$), 2 ($238 \leq SL < 687$), and 3 ($SL < 237$).

The variable resistance of different rocks highly affects the SL index. Thus, the best course of action is to use a spatial filter to evaluate the SL anomalies related to either lithology or fault movements. The filter can be obtained by analyzing the areal frequency distribution of SL values for each lithology group with similar characteristics that crop out in a drainage basin (Troiani et al. 2014); in this method, only the statistical outliers have been considered as anomalies.

Based on this method, two box-plots and histograms have been made to represent the frequency of SL values for both high- and low-strength lithological groups. These graphs show that in high-strength rock groups, the maximum frequency of lower values is low, in comparison with that in low-strength rock groups. Moreover, the mean SL value is 210 m for the high-strength rocks and 165 m for the low-
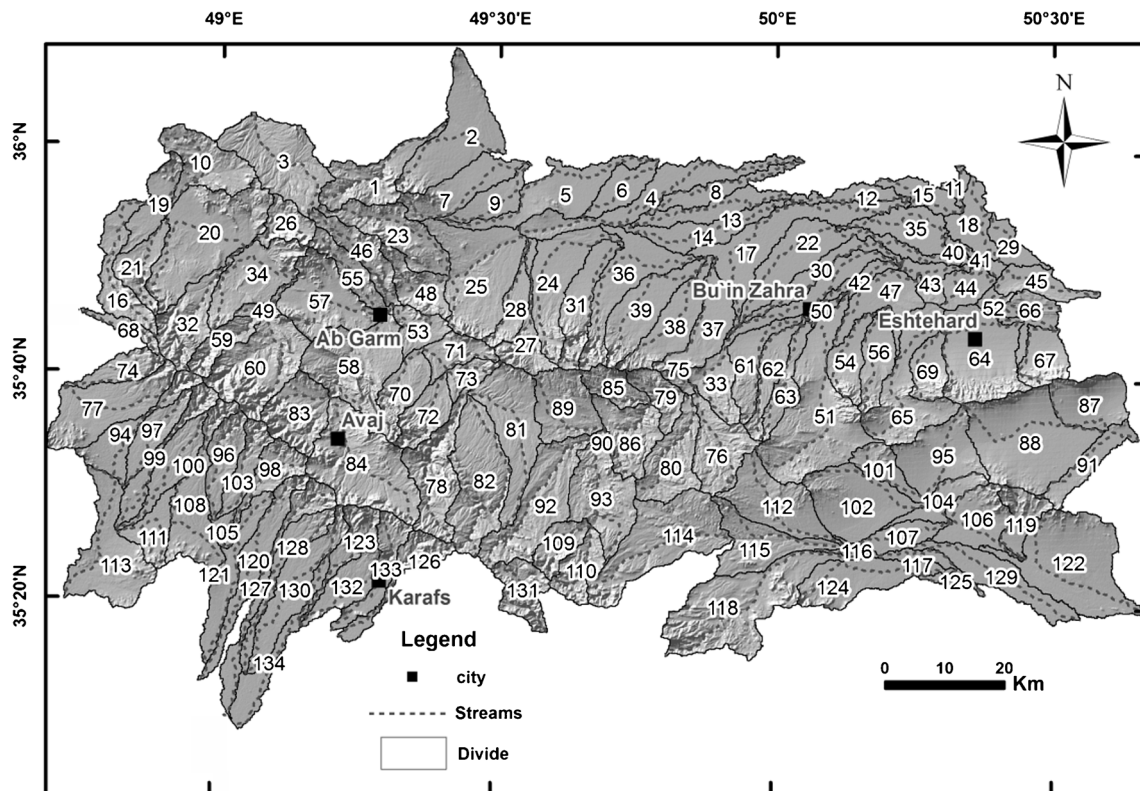
Fig. 2 Shoor river basin and its 134 sub-basins used as unit areas for the morphometric analyses

strength rocks. The maximum outlier for hard rocks is 500 and this value is 460 for weak rocks.

Likewise, we have interpolated SL values to make a surface covering along the drainage basins although they have been calculated along streams. The lithological filtering and kriging interpolation of the values, performed through the drainage network, has proved the role of active faulting on the perturbations of SL. Figure 4 represents this result. Applying these methods, we have made a map which represents SL values and main faults to help the interpretation of the anomalies. The purpose of the map is to indicate the key role of some fault segments on SL anomalies.

Asymmetry factor

The asymmetric factor (Af) is a way to evaluate the existence of tectonic tilting at the scale of a drainage basin. The method may be applied over a relatively large area (Hare and Gardner 1985; Keller and Pinter 2002). Af is defined by Eq. (2):

$$Af = 100\left(Ar\big/At\right), \qquad (2)$$

where Ar is the area of the basin to the right (facing downstream) of the trunk stream, and At is the total area of the drainage basin. If the value of this factor is close to 50, the basin has a stable condition or with little tilting,

while values above or below 50 may result from basin tilting, resulting from tectonic activity. In the study area, for the purpose of evaluating relative active tectonics, the measured Af values were employed to prepare the final Af map. Figure 7 indicates Af values that were grouped into three classes: high ($-42 \leq Af < -28$ or $28 \leq Af < 42$), moderate ($-27 \leq Af < -9$ or $9 \leq Af < 27$), and low ($-8 \leq Af < 8$). Sub-basins on the major faults such as Ipak, Soltaniyeh, Avaj, and Hasan Abad faults show the most tilting.

Hypsometric integral

The hypsometric integral is an index that describes the distribution of the elevation of a given area or a landscape (Strahler 1952). The Hi is independent of the basin area. This index is defined as the area below the hypsometric curve and thus expresses the volume of a basin that has not been eroded. A simple equation that may be used to calculate the index (Pike and Wilson 1971) is defined by Eq. (3):

Hi = (average elevation−min elevation)/(max elevation−min elevation).
(3)

Using Eq. (3), we computed Hi for each sub-basin. It ranges from 0.15 (sub-basin 19 and 43) to 0.56 (sub-basin 1). Then, Hi values were grouped into three classes:
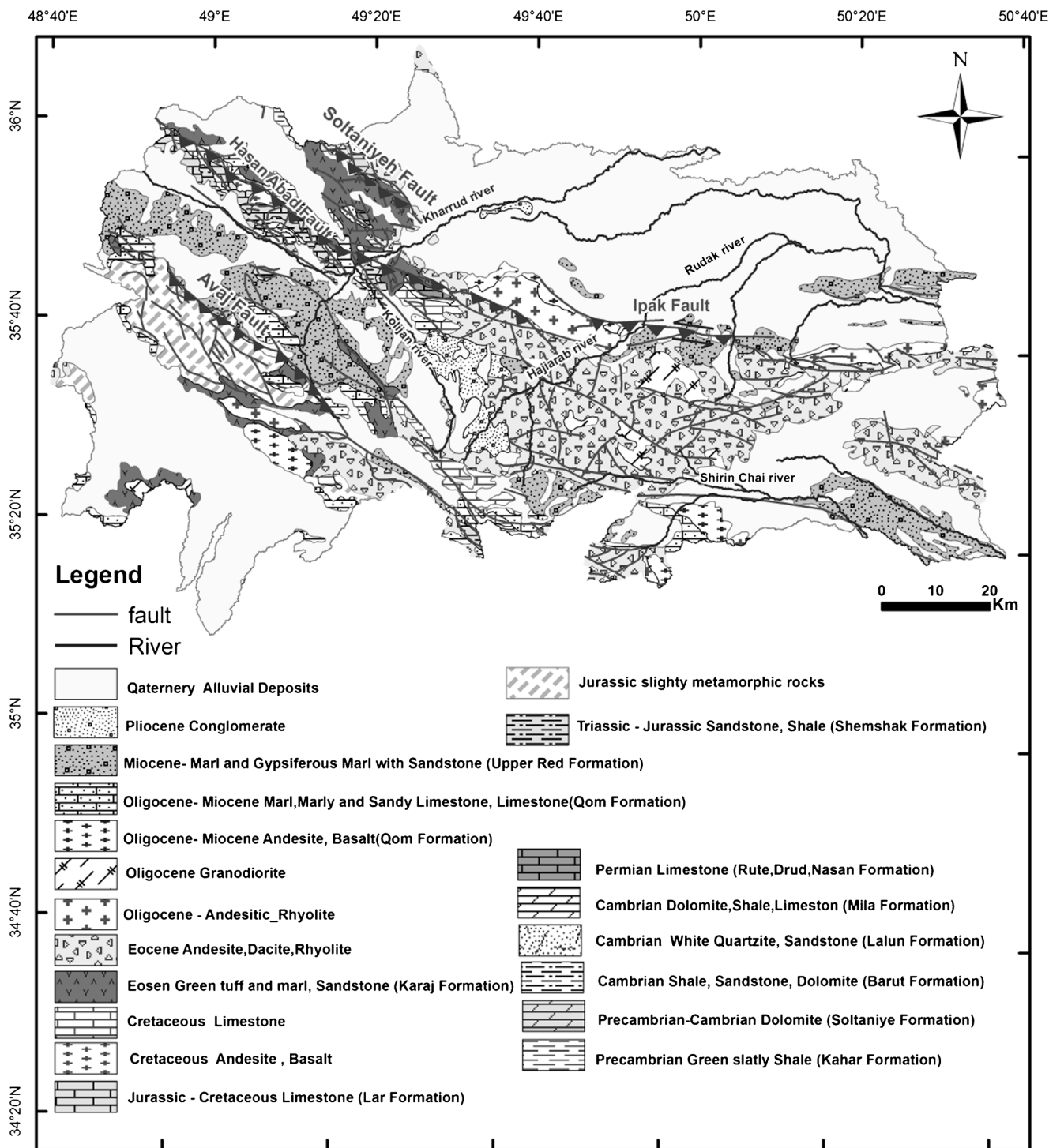
Fig. 3 Geological map of the study area

Figures 5b and 8 represent class 1 with convex hypsometric curves ($0.38 \leq Hi \leq 0.56$), class 2 with concave–convex hypsometric curves ($0.27 \leq Hi < 0.38$), and class 3 with concave hypsometric curves ($0.15 \leq Hi < 0.27$). The greatest value of this index corresponds to sub-basins Soltaniyeh and Avaj Fault zones and the sub-basins located south of the Ipak Fault zone.

Ratio of valley floor width to valley height

Vf is defined as the ratio of the width of the valley floor to its average height (Bull and McFadden 1977; Bull 1978) and is computed by Eq. (4):

$$Vf = 2Vfw / (A_{ld} + A_{rd} - 2A_{sc}) \qquad (4)$$

Fig. 4 The contour lines of SL index values in the study area
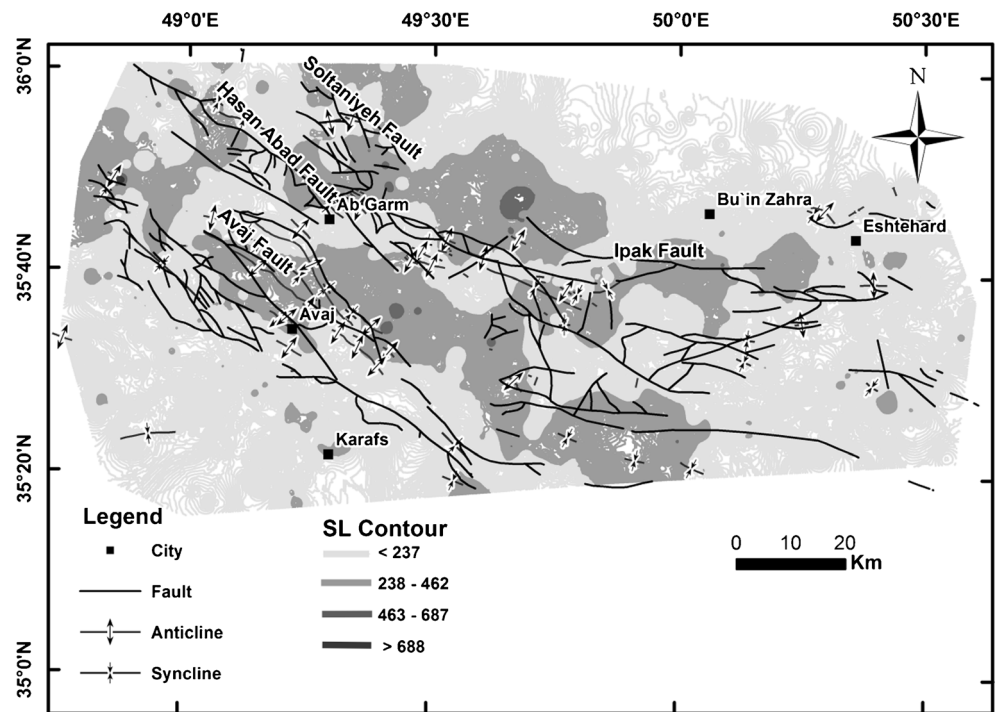
where Vfw is the width of the valley floor, and A_{ld}, A_{rd}, and A_{sc} are the altitudes of the left and right divides (looking

downstream) and the stream channel, respectively (Bull 2007). A significant relationship exists between the rate of
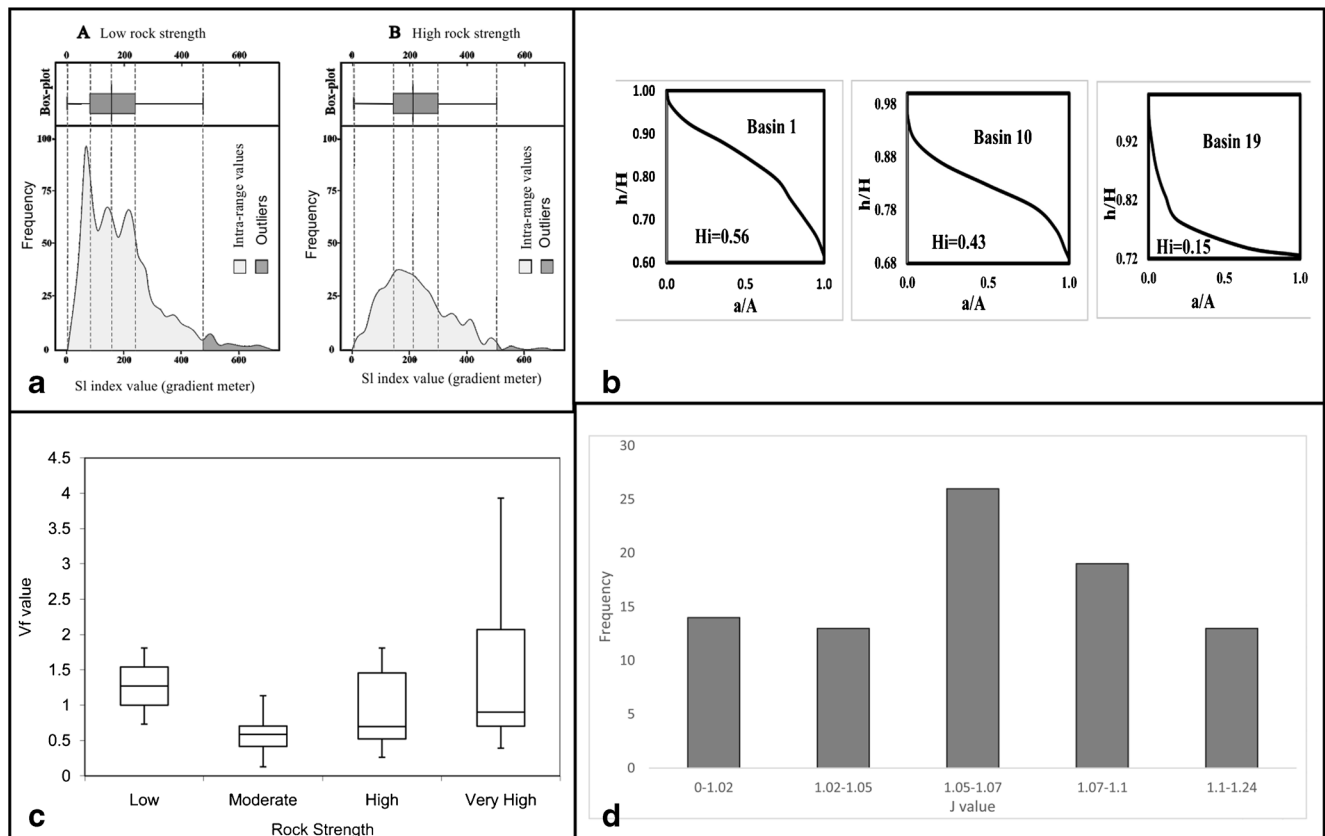

Fig. 5 **a** Frequency histograms relative to the interpolated values of SL within low rock strength (*A*) and high rock strength rock (*B*) formations. **b** Hypsometry curves of three sub-basins. **c** Box-plot of the Vf index values of the various rock strength. **d** Frequency histograms of the J index values
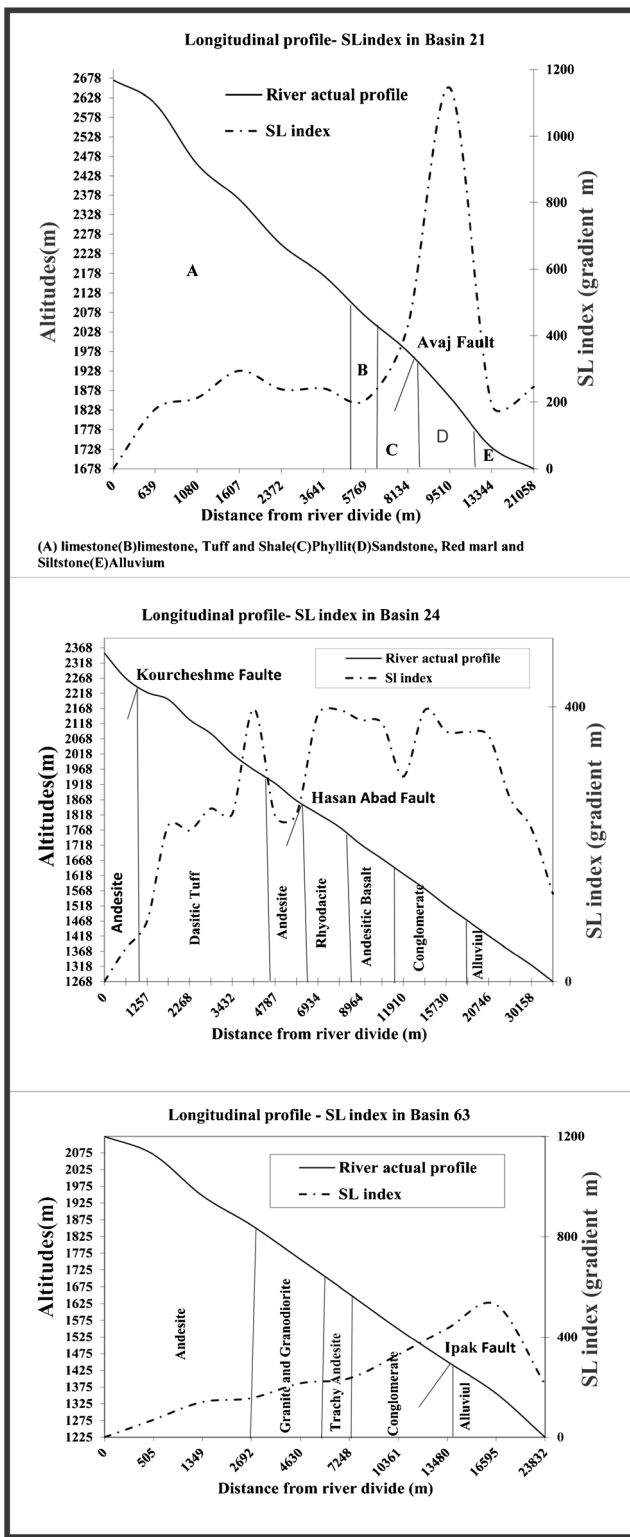
Fig. 6 Longitudinal river profiles and measured SL values for three sub-basins in this area

mountain front activity and the Vf index (Bull and McFadden 1977). Consequently, the high Vf values conform to low uplift rates (Keller and Pinter 2002). The index was originally used to distinguish V-shaped valleys from U-shaped valleys (Bull and McFadden 1977). V-shaped valleys are common in areas of active uplift and deep, linear stream incision (low Vf values). U-shaped valleys are representative of formerly glaciated or tectonically stable areas where stream valley bottoms tend to be wider (higher Vf values). Vf crosses were considered for main valleys at distances between 0.5 and 1 km from the mountain fronts using cross-sections drawn from the DEM. According to the index value in lithology with different strengths, a box diagram is shown in Fig. 5c. The range of Vf is from 0.26 (sub-basin 27) to 3.88 (sub-basin 119). Vf is relatively low for V-shape valleys but high for U-shape valleys. In this research, we study the Vf sections along the mountain fronts with the low (older alluvial fan deposit, Plio-Quaternary conglomerate), moderate (phyllite, schist, shale, marl, gypsum, and tuff), high (limestone, sandstone, dolomite, and hard conglomerate), and very high (volcanic and plutonic rocks) rock strength. The results are shown in Table 1. According to the obtained Vf values, most valleys in the study area are V-shaped.

Index of drainage basin shape

Relatively young drainage basins in active tectonic areas tend to be elongated in shape perpendicular to the topographic slope of a mountain. With continued evolution or less active tectonic processes, the elongated shape tends to evolve to a more circular shape (Bull and McFadden 1977). Horizontal projection of basin shape may be described by the elongation ratio, Bs (Cannon 1976; Ramírez-Herrera 1998), expressed by Eq. (5):

$$Bs = Bl/Bw, \qquad (5)$$

where Bl is the length of the basin measured from the headwaters to the mouth, and Bw is the width of the basin measured at its widest point. High values of Bs are associated with elongated basins, generally associated with relatively higher tectonic activity. Low values of Bs indicate a more circular-shaped basin, generally associated with low tectonic activity. Rapidly uplifted mountain fronts generally produce elongated, steep basins, and when tectonic activity is diminished or ceases, widening of the basins occur from the mountain front up (Ramírez-Herrera 1998).

Bs was computed using the DEM and classified into three classes: 3 ($1.02 \leq Bs < 2.78$), 2 ($2.78 \leq Bs < 5.07$), and 1 ($5.07 \leq Bs < 9.22$). The most elongated sub-basins with the highest values of Bs occur along the Ipak fault and Avaj fault zone shown in Fig. 9.

Index of mountain front sinuosity

Index of mountain front sinuosity (Bull and McFadden 1977; Bull 1978) is defined by Eq. (6):
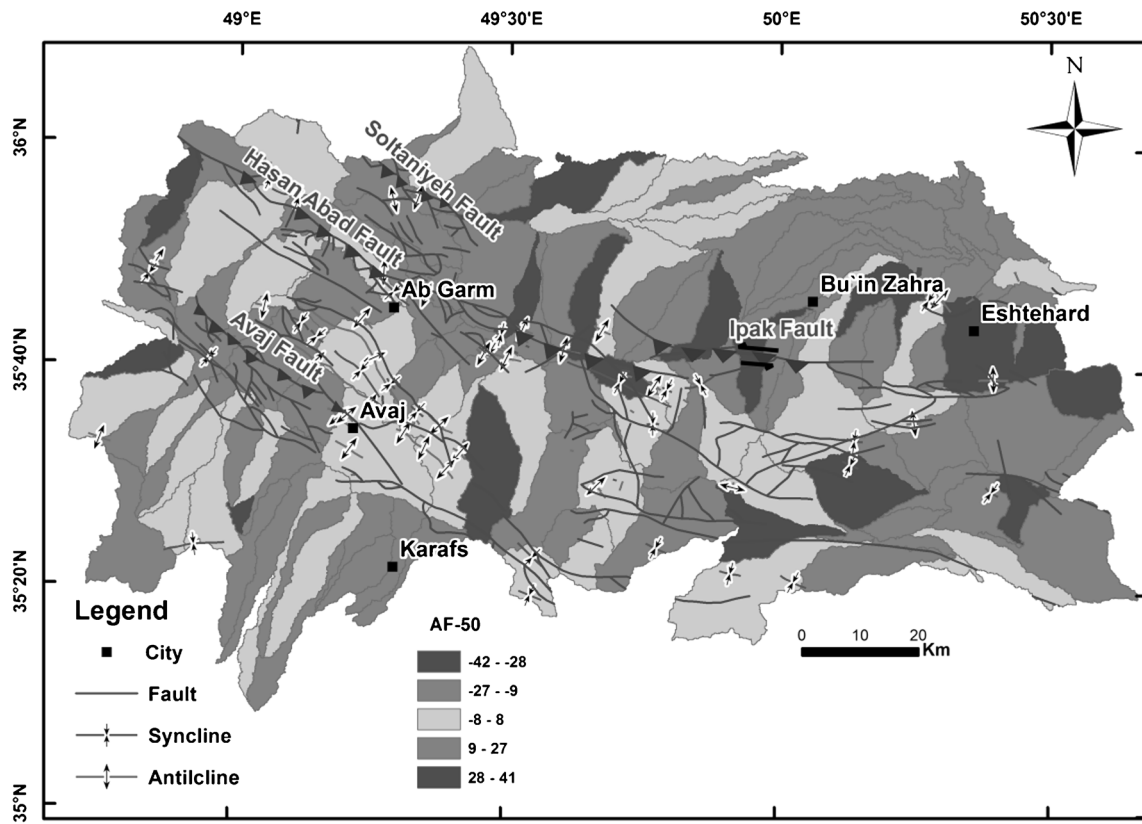
$$Smf = Lj/Ls, \qquad (6)$$
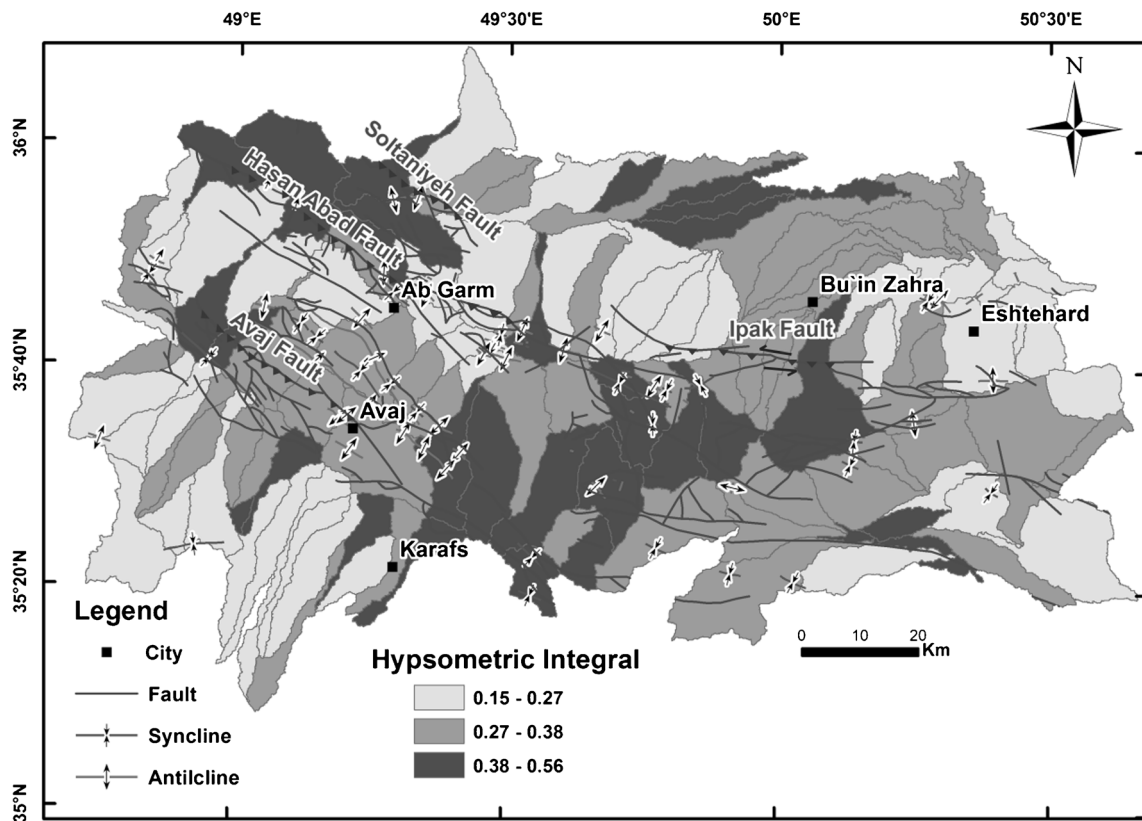
Fig. 7 Distribution of Af classes

Fig. 8 Distribution of Hi classes

Table 1 Values of At (total sub-basin area), the classes of SL (stream-gradient index), Af (drainage basin asymmetry), Hi (hypsometric integral), Vf (valley floor width–valley height ratio), Bs (drainage basin shape), and J (mountain front sinuosity) and values and classes of Iat (relative tectonic activity)

Basin no.	Class of SL[a]	Class of AF[b]	Class of Hi[c]	Class of J[d]	Class of Vf[e]	Class of Bs[f]	Value of Iat	Class of Iat[g]
1	2	2	1	1		2	1.6	1
2	3	3	3	1	1	2	2.17	3
3	3	3	1			3	2.5	4
4	3	3	2			1	2.25	3
5	3	1	3			2	2.25	3
6	3	3	1			2	2.25	3
7	3	2	2	1		2	2	2
8	3	2	1			1	1.75	1
9	3	2	2			2	2.25	3
10	3	2	1			3	2.25	3
11	3	2	1			3	2.25	3
12	3	2	1			1	1.75	1
13	3	3	1			1	2	2
14	3	3	1			1	2	2
15	3	2	2			2	2.25	3
16	2	2	2			1	1.75	1
17	3	2	2			1	2	2
18	3	2	2			3	2.5	4
19	3	1	3			2	2.25	3
20	3	3	3	1		3	2.6	4
21	2	2	3	1	2	2	2	2
22	3	2	2			1	2	2
23	2	2	1	1		2	1.6	1
24	2	2	3	1	3	2	2.17	3
25	3	2	3	1	2	3	2.33	3
26	3	2	1	1		3	2	2
27	2	2	1	1	1	2	1.5	1
28	3	1	2	1	3	2	2	2
29	3	2	3			3	2.75	4
30	3	2	2			1	2	2
31	2	1	2		2	2	1.8	1
32	2	2	1	1	2	2	1.67	1
33	3	2	2	1	2	2	2	2
34	3	3	3	1	3	3	2.67	4
35	3	2	2			2	2.25	3
36	2	3	3	2	2	2	2.33	3
37	3	1	3	2	2	2	2.17	3
38	2	2	3	2	3	2	2.33	3
39	2	2	3	2	2	2	2.17	3
40	3	2	1			2	2	2
41	3	2	2			2	2.25	3
42	3	3	1			1	2	2
43	3	2	3			3	2.75	4
44	3	2	3			3	2.75	4
45	3	3	3			2	2.75	4
46	2	2	1			2	1.75	1
47	3	1	3			3	2.5	4
48	3	2	2	1		3	2.2	3
49	3	3	2			2	2.5	4
50	3	2	2			2	2.25	3
51	2	3	1	1		2	1.8	1
52	3	2	3			3	2.75	4
53	3	2	3			3	2.75	4
54	3	2	2	1		2	2	2
55	3	3	2			2	2.5	4
56	3	2	3	1	2	2	2.17	3
57	3	2	3	1		3	2.4	3
58	3	3	2	1		3	2.4	3
59	2	2	1			2	1.75	1
60	2	2	2	1	2	3	2	2
61	3	1	2	1		2	1.8	1
62	2	2	2	1	3	1	1.83	1
63	2	2	2	1	2	2	1.83	1

Table 1 (continued)

Basin no.	Class of SL[a]	Class of AF[b]	Class of Hi[c]	Class of J[d]	Class of Vf[e]	Class of Bs[f]	Value of Iat	Class of Iat[g]
64	3	1	3	1	2	3	2.17	3
65	2	3	2	1	2	2	2	2
66	3	2	3		1	3	2.4	3
67	3	1	3	1	1	3	2	2
68	3	3	2		2	1	2.2	3
69	3	2	2	1		3	2.2	3
70	2	2	2	1	2	2	1.83	1
71	3	2	2		2	2	2.2	3
72	2	3	2	1	2	3	2.17	3
73	3	2	3	2	2	3	2.5	4
74	3	1	2	1	2	2	1.83	1
75	3	2	1			3	2.25	3
76	2	3	1			3	2.25	3
77	3	3	3	1	2	3	2.5	4
78	2	3	1	1		2	1.8	1
79	3	3	2			3	2.75	4
80	2	2	1			3	2	2
81	3	3	1	2		2	2.2	3
82	2	1	1	1		2	1.4	1
83	2	2	2	1	2	3	2	2
84	3	3	2	1		3	2.4	3
85	2	1	1			3	1.75	1
86	3	3	1	2		3	2.4	3
87	3	1	3	1	3	3	2.33	3
88	3	2	2	2		3	2.4	3
89	3	2	2	2		3	2.4	3
90	3	2	1			3	2.25	3
91	3	2	2	2	3	2	2.33	3
92	2	2	1			2	1.75	1
93	2	3	1			3	2.25	3
94	3	2	3	1	2	2	2.17	3
95	3	2	2	1		3	2.2	3
96	3	2	2	1	1	2	1.83	1
97	3	3	3	1	2	2	2.33	3
98	3	2	1	1	3	2	2	2
99	3	2	2	1	2	1	1.83	1
100	3	3	2	1		2	2.2	3
101	3	2	1	2		3	2.2	3
102	3	1	2	2		3	2.2	3
103	3	3	2	1	1	2	2	2
104	3	2	3			3	2.75	4
105	3	1	1			3	2	2
106	3	2	3	2		3	2.6	4
107	3	2	1			2	2	2
108	3	3	3	1	1	2	2.17	3
109	3	2	1			3	2.25	3
110	2	3	1			3	2.25	3
111	3	3	3			3	3	4
112	3	3	1	2		3	2.4	3
113	3	2	3			3	2.75	4
114	2	2	2			2	2	2
115	3	1	2			2	2	2
116	3	2	1			2	2	2
117	3	2	1			1	1.75	1
118	2	3	2			2	2.25	3
119	3	1	2	2	3	3	2.33	3
120	3	2	3			1	2.25	3
121	3	2	3			1	2.25	3
122	3	2	3	2	3	3	2.67	4
123	3	2	1			2	2	2
124	3	2	3			2	2.5	4
125	3	3	1			2	2.25	3
126	3	2	1	1	1	2	1.67	1
127	3	3	3			1	2.5	4
128	3	2	2			1	2	2

Table 1 (continued)

Basin no.	Class of SL[a]	Class of AF[b]	Class of Hi[c]	Class of J[d]	Class of Vf[e]	Class of Bs[f]	Value of Iat	Class of Iat[g]
129	3	3	1			1	2	2
130	3	3	3			2	2.75	4
131	3	3	1			3	2.5	4
132	3	2	3	1		2	2.2	3
133	3	2	2	1	1	2	1.83	1
134	3	2	2			1	2	2

[a] Stream-gradient index

[b] Drainage basin asymmetry index

[c] Hypsometric integral index

[d] Index of mountain front sinuosity

[e] Valley floor width-valley height ratio

[f] Index of drainage basin shape

[g] Relative tectonic activity index (Iat class is came from averaging indices)

where Lj is the length of the mountain front along the foot of the mountain where a change in slope from the mountain to the piedmont occurs, and Ls is the straight line length of the mountain front. Smf represents a balance between erosive processes tending to erode a mountain front, making it more sinuous through streams that cut laterally, and into the front and active vertical tectonics that tend to produce straight mountain fronts, often corresponding to active faults or folds (Bull and McFadden 1977). The values of Smf were calculated for 31 mountain fronts, using Lj and Ls values measured from topographic maps (1:25,000); Fig. 5d represents all the observed values that are between 1.02 and 1.24 and belong to classes 1 and 2. Smf values reflect the existence of straight mountain fronts in the study area and thus active tectonics of mountain front.

Evaluation of relative tectonic activity

Previous studies on relative tectonic activity based on geomorphic indices tend to focus on a particular mountain front or area (Bull and McFadden 1977; Rockwell et al. 1985; Azor et al. 2002). This study tried to evaluate tectonics in a wider area, using a number of geomorphological parameters. The average of the six measured geomorphic indices (Iat) was used to evaluate the distribution of relative tectonic activity in the study area. The values of the index were divided into four classes to define the degree of active tectonics: (1) very high ($1.4 \leq$ Iat < 1.8), (2) high ($1.8 \leq$ Iat < 2.0), (3) moderate ($2.0 \leq$ Iat < 2.4), and (4) low ($2.4 \leq$ Iat < 3). The distribution of the four classes is shown in Fig. 10, and Table 1 shows the result of the classification for each sub-basin. About 18% of the study area (about 2066 km^2) belongs to class 1, 20% (2362 km^2) to class 2, 44% (5087 km^2) to class 3, and 18% (2158 km^2) to class 4.

Discussion

The tectonic mobility of the Alborz is due to the northward movement of the central Iran, as well as the northwestward movement of the South Caspian Basin (Vernant et al. 2004b; Ritz et al. 2006). The contemporaneous presence of these two mechanisms resulted in the creation of a transpressional regime (with NNE-SSW trend) in the Alborz, which has begun 5 ± 2 Ma ago (Jackson and McKenzie 1984; Ritz et al. 2006). The neotectonic investigations show that the current deformation in the Alborz is divided along the thrust and sinistral strike-slip faults (Jackson et al. 2002; Allen et al. 2003; Ritz et al. 2006). The study area, located in both Alborz and the central Iran, is affected by these deformations, and its overall tectonics completely follows Alborz orogeny. The central Alborz records the highest uplift rate on the southern edge (Ballato et al. 2013). This research, likewise, presents that the most uplift has occurred during the neotectonic regime (Ballato et al. 2013). The assessment of Quaternary kinematics shows that vertical movements often focus on the southern edge of the central Alborz (Ballato et al. 2013). In this study, it is found that there exists a high relative tectonic activity along the fault zones based on the index of active tectonics (Iat), which has had a significant impact on the current topography and landform creation according to field evidences. The Soltaniyeh fault, which is one of the main faults in the northwestern part of the study area, has the northwest-southeast strike and southwest deep and shows a reverse dextral strike-slip movement. According to the Iat classification, this fault has played an important role in this region by presenting the very high amount of recent tectonic activity. Thus, basins 1 and 23 that are situated along its southeastern termination, in the overlap area (step over) between this fault and
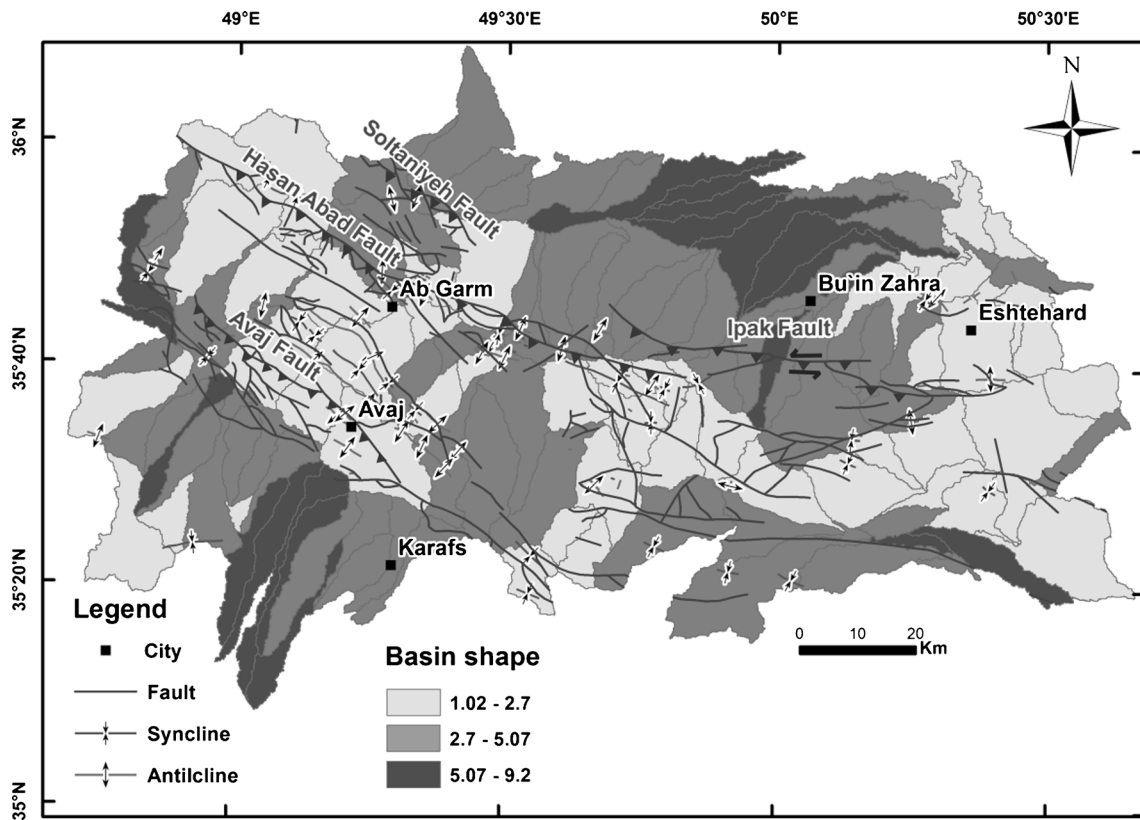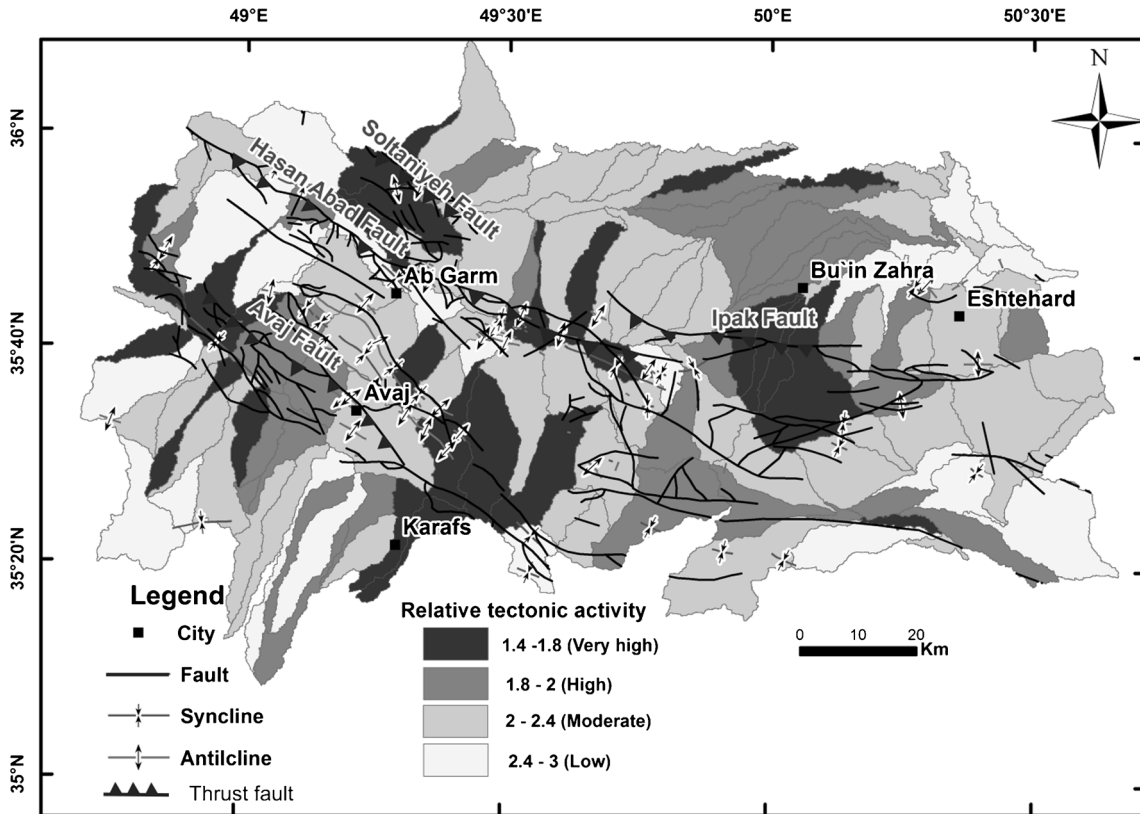
Fig. 9 Distribution of Bs classes
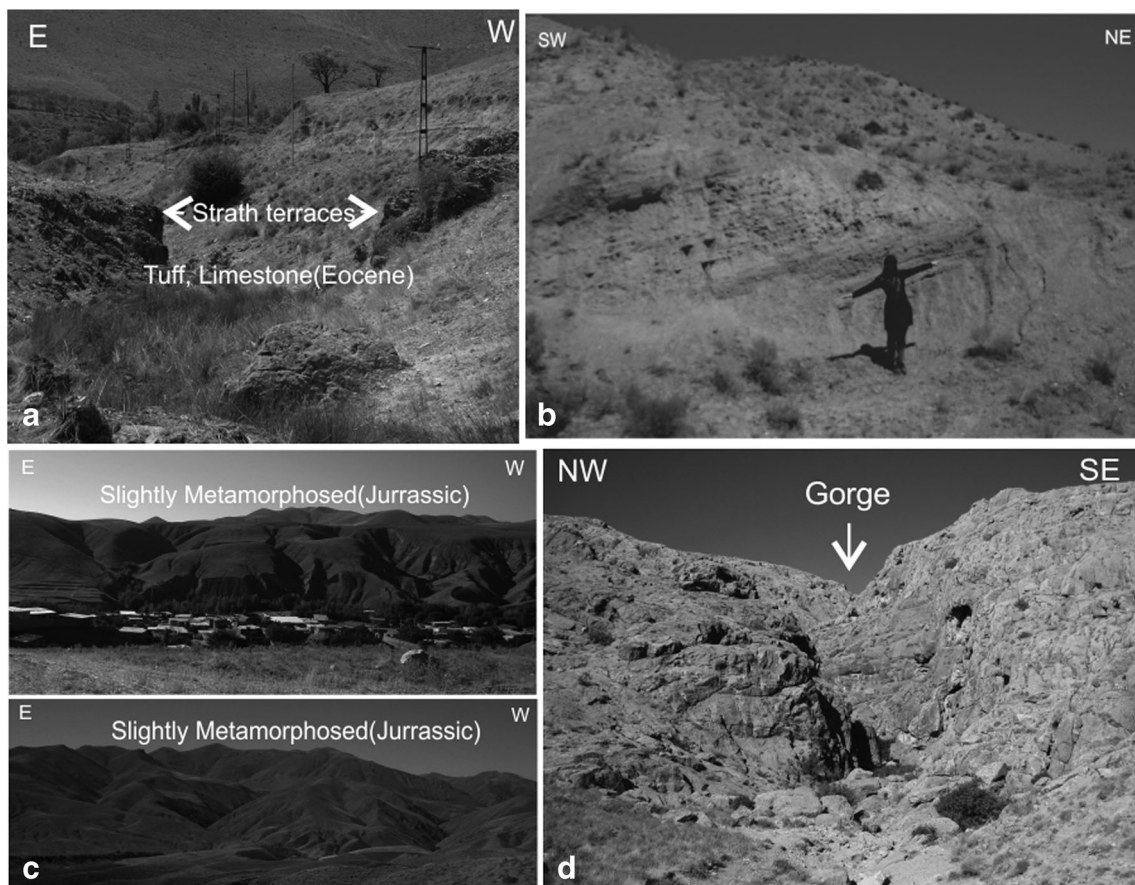

Fig. 10 Distribution of Iat classes

Fig. 11 **a** Strath terraces as a result of getting drilled Bedrock by the river in the south of the Ipak fault. **b** Quaternary units tilting along the Avaj fault. **c** V-shaped valleys in the north of the Avaj fault. **d** Gorge in the northwestern Avaj fault zone

the west sector of the Hasan Abad left-lateral reverse fault, show class 1 of the active tectonics. The Soltaniyeh earthquake, which occurred in 1803, was probably due to the activity of this fault. Therefore, based on this earthquake as well as on the high value of Iat on this fault, it can be said that the Soltaniyeh fault is one of the current active faults which should be taken into account in seismotectonic studies. Additionally, the value of Iat in sub-basins 27 and 31, situated in the step over area between the southeast part of the Hasan Abad fault and the west end of the Ipak reverse fault, also falls into class 1. This claim is corroborated by the landform evidences obtained from the field studies, such as deep V-shaped valleys and the strath terraces which are resulted from the river bedrock graving through uplift, indicated in Fig. 11a. Based on the Iat classification map, very high and high tectonic activities (class 1 and 2) are observed on the Ipak reverse fault and some segments of the Hasan Abad fault zone. The Ipak reverse fault with small sinistral strike-slip component (Ambraseys 1963; Berberian 1976) with 100 km length and west–east strike passes south of Buin Zahra. The high amount of the stream length-gradient index (SL) and straight mountain fronts along this fault

indicate the high tectonic activity through the mentioned fault. In the southern of Buin Zahra, some segments of the Ipak Fault zone have affected the Quaternary units and have tilted them severely, so the Af index shows high positive tilting in this part. Furthermore, field data indicate the significant tilting in all existing river basins toward the west and northwest because of the recent active tectonics through the Ipak fault zone.

Another important fault zone in the study area is the Avaj fault zone with northwest–southeast strike which is situated in the west and southwest parts of the study area. Almost all basins, located in this fault zone, show relatively very high and high tectonic activities (class 1 and 2). Since this fault zone caused the tilting of Quaternary units, it has been active over the Quaternary, represented in Fig. 11b. The Changureh earthquake occurred due to the activity of one of this fault zone segments. Figure 11c, d shows the field evidences such as the deep V-shaped valleys and gorges, on the hanging wall of Avaj fault, confirm the recent tectonic activity along the other fault segments of this zone. The high values of Iat index in this part of the region as well as the occurrence of the numerous earthquakes along some segments of the Avaj fault zone can prove the existence of high recent tectonic activity.

Fig. 12 V-shaped valleys on the footwall of the North Avaj fault-related uplift

Fig. 13 Cut and tilting alluvial fan deposits and terraces Quaternary around town Karafs

This fault zone, in the most part of its length, has caused the thrusting of the Jurassic metamorphic rocks in the southwest part on the Miocene sandstone and marl in the northeast part. In some parts of the Avaj fault zone, the rivers have incised sandstone and conglomerate units as narrow deep valleys on the footwall of the North Avaj fault zone which represent the high uplift rate in these regions that is obvious in Fig. 12. The obtained field evidence from sub-basins around Karafs, in the southeastern part of the study area, characterizes the cutting and tilting of the Quaternary units, indicating the recent tectonic activity on the foot wall of south Avaj fault zone which is clear in Fig. 13. In some fault zones, through some fault segments, there exist some low SL anomalies due to the fact that those faults only represent the strike-slip movements without any dip-slip activities and vertical changes. However, higher anomalies have been represented through the rivers and thrust faults with high amount of vertical movements. U-shaped valleys show tectonically inactive valleys where their bottoms tend to be wider (higher Vf values). Nevertheless, in some fault zones such as Ipak, there exist several wide valley floors
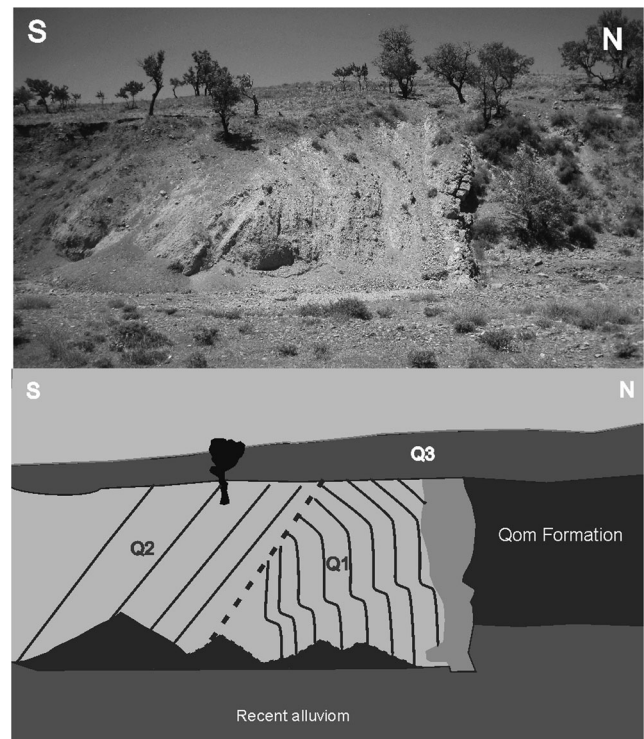
through active fault segments due to their strike-slip movements. As strike-slip movements tend to crush the rocks and increase the width of the valley floors, they may make U-shaped valleys through some fault segments although they are active.

On the other hand, the lowest Iat values (class 4) mainly occur in the eastern and northeastern parts of the study area, where all geomorphic indices suggest low tectonic activity. This could be related to the vast plains associated with inactive syncline fold axes.

The lack of earthquake through some main fault segments limits the possibility of seismic hazard evaluation. Therefore, by using this method, we have been able to indicate that some main fault segments, such as the Soltaniyeh fault; most segments of the Ipak fault zone; and the stop over area between the Hasan Abad fault and the Ipak fault represent high relative tectonic activity which means that they are capable of creating earthquakes in the future.

Conclusions

According to the Iat classification, 82% of the study area shows very high to moderate level of relative tectonic activity. The values of SL, Hi, and Bs were found to be high along the Soltaniyeh, Avaj, Hasan Abad, and Ipak fault segments. The lithological filtering and kriging interpolation of the SL values, performed along the drainage network, has proved

the important role of active faults on the increase of this index. The values of Af show widespread drainage basin asymmetry related to the tectonic tilting, particularly associated with Ipak fault. The values of smf suggest that nearly all mountain fronts are tectonically active, and the values of Vf show that some valleys are narrow and deep, suggesting a high rate of incision. The parts with class 1 and 2 of the relative tectonic activity are located along the main faults of the study area, such as Soltaniyeh, Avaj, Hasan Abad, and Ipak faults, and show high correlation with observed landforms during the field investigations such as the straight mountain fronts, fault gorges, fault scarps, and deep V-shaped valleys. Besides, the high amount of the relative tectonic activity index (Iat) shows a good fit with the tilting and deformation of the Quaternary units, which are resulted from the effect of compressive stresses affecting the region. These stresses are caused by the movement of the Arabian plate towards the Iranian plateau and the structures with NNW–SSE are formed due to the same stress. In general, the parameters used in this study show the sensitivity of these indices to the tectonic activity. These parameters can be considered as a valid evidence to prove the existence of the recent tectonic movements in some main fault segments which had not been considered active before.

References

Allen MB, Armstrong HA (2008) Arabia-Eurasia collision and the forcing of mid-Cenozoic global cooling. Palaeogeogr Palaeoclimatol Palaeoecol 265:52–58. doi:10.1016/j.palaeo.2008.04.021

Allen MB, Ghassemi MR, Sharabi M, Qoraishi M (2003) Accommodation of late Cenozoic oblique shortening in the Alborz range, northern Iran. J Struct Geol 25:659–672. doi:10.1016/S0191-8141(02)00064-0

Allen M, Jackson J, Walker R (2004) Late Cenozoic reorganization of the Arabia- Eurasia collision and the comparison of short-term and long term deformation rates. Tectonics 23:153–165. doi:10.1029/2003TC001530

Ambraseys NN (1963) The Buyin-Zara (Iran) earthquake of September, 1962 a field report. Bull Seismol Soc Am 53:705–740

Azor A, Keller EA, Yeats RS (2002) Geomorphic indicators of active fold growth: South Mountain–Oak Ridge Ventura basin, Southern California. Geol Soc Am Bull 114:745–753. doi:10.1130/0016-7606(2002)114<0745:G

Ballato P, Stockli DF, Ghassemi MR, Landgraf A, Strecker MR, Hassanzadeh J, Friedrich A, Tabatabaei SH (2013) Transpressional tectonics in the Arabia–Eurasia collision zone: new constraints from (U–Th)/He thermochronology in the Alborz Mountains, N Iran. Tectonics 32(1):1–18. doi:10.1029/2012TC003159

Berberian M (1976) An explanatory note on the first seismotectonic map of Iran; a seismo-tectonic review of the country. In: Contribution to the seismotectonics of Iran (Part II). Geological Survey of Iran, 518p

Berberian M (1983) The southern Caspian: a compressional depression floored by a trapped, modified oceanic crust. Can J Earth Sci 20:163–183. doi:10.1139/e83-015

Berberian M, King GCP (1981) Towards a paleogeography and tectonic evolution of Iran. Can J Earth Sci 18:210–265

Berberian M, Yeats RS (2001) Contribution of archeological data to studies of earthquake history in the Iranian plateau. J Struct Geol 23:563–584. doi:10.1016/S0191-8141(00)00115-2

Berberian M, Qorashi M, Arzhang-ravesh B, Mohajer-Ashjai A (1993) Recent tectonics, seismotectonics and earthquake fault hazard investigations in the Greater Tehran region: contribution to the seismotectonics of Iran, part V, Geological Survey of Iran, Report 56, 316p

Bull WB (1978) Geomorphic tectonic classes of the south front of the San Gabriel mountains, California. U.S. Geological Survey Contract Report, 14–08-001-G-394, Office of Earthquakes, Volcanoes and Engineering, Menlo Park, CA

Bull WB (2007) Tectonic geomorphology of mountains: a new approach to paleoseismology. Blackwell, Malden

Bull WB, McFadden LD (1977) Tectonic geomorphology north and south of the Garlock fault, California. In: Doehring DO (ed) Geomorphology in Arid Regions. Proceedings of the Eighth Annual Geomorphology Symposium. State University of New York, Binghamton, 115–138

Cannon PJ (1976) Generation of explicit parameters for a quantitative geomorphic study of Mill Creek drainage basin. Oklahoma Geology Notes 36(1):3–16

Cox RT (1994) Analysis of drainage-basins symmetry as rapid technique to identify areas of possible Quaternary tilt-block tectonics: an example from Mississippi embayment. Geol Soc Am Bull 106:571–581. doi:10.1130/0016-7606(1994)106<0571:A

Dehbozorgi M, Pourkermani M, Arian M, Matkan AA, Motamedi H, Hosseinias H (2010) Quantitative analysis of relative tectonic activity in the Sarvestan area, central Zagros, Iran. Geomorphplogy 13:243–360. doi:10.1016/j.geomorph.2010.05.002

Della Seta M (2004) Azimuthal transects of stream orientations: an advance in understanding the regional morphotectonic setting of eastern Abruzzo (central Italy). Geogr Fis Din Quat 27(1):21–28

Della Seta M, Del Monte M, Fredi P, LupiaPalmieri E (2004) Quantitative morphotectonic analysis as a tool for detecting deformation patterns in soft rock terrains: a case study from the southern marches, Italy. Géomorphologie: Relief, Processus, Environnement 4:267–284

Della Seta M, Del Monte M, Fredi P, Miccadei E, Nesci O, Pambianchi G, Piacentini T, Troiani F (2008) Morphotectonic evolution of the Adriatic piedmont of the Apennines: advancement in the knowledge of the Marche–Abruzzo border area. Geomorphology 102:119–129. doi:10.1016/j.geomorph.2007.06.018

Hack JT (1973) Stream-profiles analysis and stream-gradient index. Journal of Research of the US Geological Survey 1:421–429

Hare PW, Gardner TW (1985) Geomorphic indicators of vertical neotectonism along converging plate margins, Nicoya Peninsula, Costa Rica. In: Morisawa M, Hack JT (eds) Tectonic Geomorphology. Proceedings of the 15th Annual Binghamton Geomorphology Symposium. Allen and Unwin, Boston, pp123–134

Jackson J, McKenzie D (1984) Active tectonics of the Alpine-Himalayan Belt between western Turkey and Pakistan. Geophys J R Astron Soc 77:185–264. doi:10.1111/j.1365-246X.1984.tb01931.x

Jackson J, Priestley K, Allen M, Berberian M (2002) Active tectonics of the South Caspian Basin. Geophys J Int 148:214–245. doi:10.1046/j.1365-246X.2002.01588.x

Keller EA, Pinter N (1996) Active tectonics: earthquakes, uplift, and landscape. Prentice Hall, New Jersey

Keller EA, Pinter N (2002) Active tectonics: earthquakes, uplift, and landscape, 2nd edn. Prentice Hall, New Jersey

Pike RJ (2002) A bibliography of terrain modeling (geomorphometry), the quantitative representation of topography. OF 02–465. U.S. Geological Survey, Menlo Park

Pike RJ, Wilson SE (1971) Elevation–relief ratio, hypsometric integral and geomorphic area–altitude analysis. Geol Soc Am Bull 82:1079–1084. doi:10.1130/0016-7606(1971)82[1079:ERH

Ramírez-Herrera MT (1998) Geomorphic assessment of active tectonics in the AcambayGraben, Mexican volcanic belt. Earth Surf Process Landf 23:317–332

Ritz JF, Nazari H, Salamati R, Shafeii A, Solaymani S, Vernant P (2006) Active transtension inside central Alborz: a new insight into the northern Iran–southern Caspian geodynamics. Geology 34:477–480. doi:10.1130/G22319.1

Rockwell TK, Keller EA, Johnson DL (1985) Tectonic geomorphology of alluvial fans and mountain fronts near Ventura, California. In: Morisawa M (ed) Tectonic Geomorphology. Proceedings of the 15th Annual Geomorphology Symposium. Allen and Unwin Publishers, Boston, pp183–207

Silva PG, Goy JL, Zazo C, Bardajm T (2003) Fault generated mountain fronts in southeast Spain: geomorphologic assessment of tectonic and earthquake activity. Gemorphology 250:203–226. doi:10.1016/S0169-555X(02)00215-5

Strahler AN (1952) Hypsometric (area–altitude) analysis of erosional topography. Geol Soc Am Bull 63:1117–1142. doi:10.1130/0016-7606(1952)63[1117: HAAOET]2.0.CO;2

Troiani F, Galveb JP, Piacentinic D, Della Setad M, Guerrerob J (2014) Spatial analysis of stream length-gradient (SL) index for detecting hillslope processes: a case of the Gállego River headwaters (central Pyrenees, Spain). Geomorphology 214:183–197. doi:10.1016/j.geomorph.2014.02.004

Vernant P, Nilforoushan F, Hatzfeld D, Abbassi MR, Vigny C, Massona F, Nankalib H, Martinod J, Ashtiani A, Bayer R, Tavakoli F, Chéry J (2004a) Contemporary crustal deformation and plate kinematics in Middle East constrained by GPS measurements in Iran and northern Oman. Geophys J Int 157:381–398. doi:10.1111/j.1365-246X.2004.02222.x

Vernant P, Nilforoushan F, Chéry J, Bayer R, Djamour Y, Massona F, Nankalib H, Ritz JF, Sedighi M, Tavakoli F (2004b) Deciphering oblique shortening of central Alborz in Iran using. Earth Planet Sci Lett 223:177–185. doi:10.1016/j.epsl.2004.04.017